

# Aggregate formation and its effect on (opto)electronic properties of guest-host organic semiconductors

Whitney E. B. Shepherd,<sup>1</sup> Andrew D. Platt,<sup>1</sup> David Hofer,<sup>1</sup> Oksana Ostroverkhova,<sup>1,a)</sup> Marsha Loth,<sup>2</sup> and John E. Anthony<sup>2</sup>

<sup>1</sup>Department of Physics, Oregon State University, Corvallis, Oregon 97331, USA

<sup>2</sup>Department of Chemistry, University of Kentucky, Lexington, Kentucky 40506, USA

(Received 3 September 2010; accepted 29 September 2010; published online 22 October 2010)

We quantify guest molecule aggregation and its effect on the photoconductive properties of guest-host thin films, depending on the guest concentration and host material. A high-performance anthradithiophene (ADT) derivative served as a guest, while functionalized benzothiophene (BTBTB) and polymethylmethacrylate (PMMA) were chosen as hosts. Aggregates exhibited redshifted optical absorption and photoluminescence (PL) spectra, as well as reduced PL quantum yields. Propensity toward guest aggregation differed for PMMA and BTBTB hosts. Photocurrents dramatically increased as the percentage of aggregated guest molecules increased due to considerably higher charge carrier mobility in the aggregates. At low guest concentrations, BTBTB films outperformed PMMA films. © 2010 American Institute of Physics. [doi:10.1063/1.3505493]

Organic (opto)electronic materials present a promising system due to their tunable properties and low cost.<sup>1</sup> Solution processable materials provide further advantages as they can be deposited using various thin-film solution deposition technologies.<sup>2</sup> Additionally, such materials can be easily doped to create blends with properties tailored for specific applications. Functionalized fluorinated anthradithiophene (ADT) derivatives are particularly interesting as their solution-deposited thin films exhibit charge carrier (hole) mobilities of  $>1.2 \text{ cm}^2/(\text{V s})$ ,<sup>3,4</sup> fast charge carrier photogeneration, high photoconductivity, and relatively strong photoluminescence (PL).<sup>5-7</sup> These molecules form  $\pi$ -stacked arrangements with short interplanar spacings of 3.2–3.4 Å,<sup>8</sup> conducive to molecular aggregate formation.<sup>9</sup> Thus, the optical and electronic properties of ADT thin films and crystals are highly sensitive to molecular packing and intermolecular interactions,<sup>5,8,10</sup> which are currently not well understood. In this letter, we seek to establish properties of ADT aggregates and conditions of their formation. In particular, we embedded ADT molecules at various concentrations into two different inert host materials and measured optical absorption, PL spectra, time-resolved PL decay dynamics, and photoconductivity upon photoexcitation of the ADT guest. These were then compared to properties of pristine ADT films.

The materials used in our studies are a fluorinated ADT derivative functionalized with triethylsilylethynyl (TES) side groups, ADT-TES-F (inset of Fig. 1),<sup>3,5</sup> as a guest, and functionalized benzothiophene (6,12-bis[2-(t-butyl)ethynyl]-benzo[1,2-b:4,5-b']bis(1)benzothiophene, t-bu BTBTB in the inset of Fig. 1) or polymethylmethacrylate (PMMA) as hosts. PMMA (Polysciences, Inc., 75,000 MW) and t-bu-BTBTB were dissolved in toluene and in tetrahydrofuran (THF), respectively, at concentrations of  $10^{-3} \text{ M}$  and  $10^{-2} \text{ M}$ , respectively. ADT-TES-F  $10^{-5} \text{ M}$  stock solutions in toluene or THF were used to add an appropriate amount of ADT-TES-F to PMMA or t-bu BTBTB solutions. PMMA (t-bu BTBTB) samples were spin coated at 600 (1000) rpm for 50 s onto clean glass substrates. Samples with several concentrations of ADT-TES-F in host matrices (PMMA and t-bu BTBTB)

were prepared, with average distances  $r$  between ADT-TES-F molecules ranging from  $r=1 \text{ nm}$  to  $r=15 \text{ nm}$ , denoted as  $P_r$  and  $B_r$ , respectively, with  $r$  in nanometers (nm). The distance  $r$  was determined according to  $r = [M/(N_A \rho_m c)]^{1/3}$ , where  $\rho_m$  is the mass density,  $M$  is the molar mass of the host material,  $N_A$  is Avogadro's number, and  $c$  is the molar fraction of guest to host.<sup>11-13</sup> Pristine ADT-TES-F films were spin coated from a  $10^{-2} \text{ M}$  toluene solution. The choice of host materials was based upon following two considerations: (1) both t-bu BTBTB and PMMA have considerably higher highest occupied molecular orbital (HOMO)-lowest unoccupied molecular orbital (LUMO) gaps (5.6 eV and 3.52 eV, respectively)<sup>14,15</sup> than that of ADT-TES-F (2.3 eV),<sup>5</sup> which minimized guest-to-host charge and energy transfer, and (2) these hosts provided different environments for embedded ADT-TES-F molecules. In particular, a t-bu BTBTB solid exhibits  $\pi$ -stacking properties similar to those of ADT-TES-F, which could impose packing constraints on embedded ADT-TES-F guest molecules. Additionally, pristine t-bu BTBTB thin films were shown to be photoconductive under 355 nm excitation.<sup>15</sup> In contrast, PMMA is not conductive and, additionally, ADT-TES-F molecules in PMMA are expected to be randomly oriented.<sup>12,16</sup> Guest concentrations in both PMMA and t-bu BTBTB hosts corresponding to  $r=1 \text{ nm}$ , 2 nm, 3 nm, 5 nm, 10 nm, and 15 nm are 1.6 mol/l, 0.2 mol/l, 0.059 mol/l,

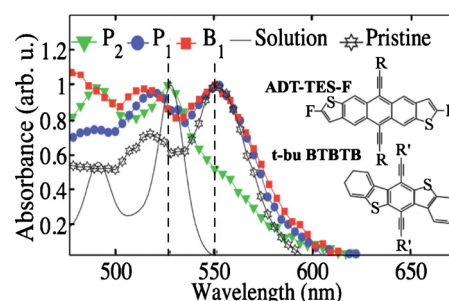


FIG. 1. (Color online) Absorbance of  $P_1$ ,  $B_1$ , and pristine ADT-TES-F films normalized by their values at 553 nm and of  $P_2$  and of ADT-TES-F solution in toluene normalized by their values at 528 nm. Dashed lines indicate dominant peak positions for the pristine film and solution. Insets show molecular structures of ADT-TES-F and t-bu BTBTB.

<sup>a)</sup>Electronic mail: oksana@science.oregonstate.edu.

0.0128 mol/l, 0.0016 mol/l, and  $4.74 \times 10^{-4}$  mol/l, respectively.<sup>12</sup> Optical densities in all films did not exceed 0.25 at the absorption maximum. For studies of photoconductivity, films were prepared on glass substrates with photolithographically deposited 5 nm/50 nm thick Cr/Au interdigitated electrode pairs. Electrodes consisted of ten pairs of 1 mm long fingers with 25  $\mu\text{m}$  finger width and 25  $\mu\text{m}$  gaps between the fingers of opposite electrodes. All experiments were carried out in air at room temperature.

Figure 1 shows optical absorption spectra of ADT-TES-F molecules in dilute toluene solution and in  $P_1$ ,  $P_2$ , and  $B_1$ , as well as pristine ADT-TES-F films. Spectrum of isolated ADT-TES-F molecules exhibits a  $0 \rightarrow 0$  transition at 528 nm with a full width at half maximum (FWHM) of  $\sim 550 \text{ cm}^{-1}$  and vibronic progression with a wave number of  $\sim 1410 \text{ cm}^{-1}$  corresponding to a C–C stretching mode.<sup>17</sup> Upon increase in guest concentration, effects of intermolecular interactions between ADT-TES-F molecules started contributing to absorption spectra.<sup>18,19</sup> In particular, an absorption band, redshifted by  $\sim 760 \text{ cm}^{-1}$  ( $\sim 25 \text{ nm}$ ) with respect to  $0 \rightarrow 0$  transition in solution, develops. This suggests an increased conjugation path leading to a higher degree of exciton delocalization.<sup>20</sup> For example, in the  $P_2$  film in Fig. 1, the band due to ADT-TES-F aggregates is seen as a shoulder at  $\sim 550\text{--}555 \text{ nm}$ , which then develops into a well-resolved peak in the  $P_1$ ,  $B_1$ , and pristine ADT-TES-F samples, while spectral features pertaining to noninteracting ADT-TES-F molecules disappear. The ADT-TES-F aggregate absorption spectrum retains exciton-phonon coupling features of isolated ADT-TES-F molecules, although most coupling occurs to a different vibrational mode with a wave number of  $\sim 1240 \text{ cm}^{-1}$  with vibronic peaks broadened (FWHM of  $\sim 900 \text{ cm}^{-1}$  and  $\sim 1000 \text{ cm}^{-1}$  in  $P_1$  and  $B_1$ , respectively) due to disorder and coupling to additional vibrational modes,<sup>21,22</sup> as compared to isolated ADT-TES-F molecules.

PL spectra of films were obtained using a 532 nm Nd:YVO<sub>4</sub> cw laser or 355 nm frequency-tripled neodymium-doped yttrium aluminum garnet pulsed excitation. In PMMA films, PL spectra did not depend on the excitation wavelength. In t-bu BTBTB films, only a 532 nm excitation was used to ensure excitation of ADT-TES-F exclusively.<sup>15</sup> Emission was collected with a parabolic mirror and detected with a fiber coupled spectrometer (Ocean Optics USB2000) calibrated against a 3100 K black-body emitter. PL lifetimes were obtained under 400 nm 80 fs excitation (frequency-doubled Ti:sapphire laser) using time-correlated single-photon counting board and an avalanche photodiode with an instrument response time of  $\sim 250 \text{ ps}$ .<sup>5</sup> Figure 2(a) shows PL spectra, corrected for self-absorption, of  $P_{15}$ ,  $B_5$ ,  $P_2$ ,  $B_2$ , and  $P_1$  films. In PMMA films at ADT-TES-F concentrations corresponding to  $r > 5 \text{ nm}$ , PL properties were similar to those of isolated (noninteracting) ADT-TES-F molecules in solution: a dominant  $0 \rightarrow 0$  transition at  $\sim 535 \text{ nm}$  followed by a vibronic progression [e.g.,  $P_{15}$  in Fig. 2(a)], single-exponential PL decays [e.g.,  $P_{10}$  in Fig. 2(b)], and high PL quantum yields (QYs) approaching 0.9. In similar t-bu BTBTB films, the shape of the PL spectra was similar to that in PMMA ones, except for a redshift by  $\sim 180 \text{ cm}^{-1}$  due to a difference in refractive indices of PMMA and t-bu BTBTB. Upon increase of ADT-TES-F concentrations, a redshifted PL band with a dominant peak at  $\sim 585 \text{ nm}$  appeared due to ADT-TES-F aggregates. For example, in Fig. 2(a),

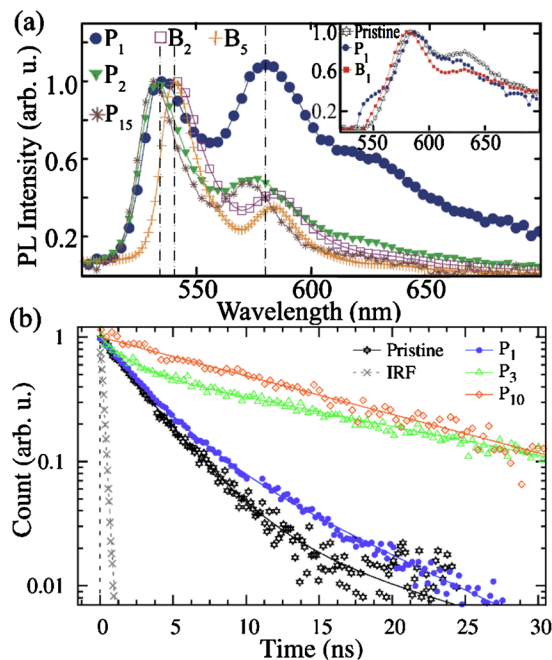


FIG. 2. (Color online) (a) PL spectra from  $P_1$ ,  $P_2$ ,  $P_{15}$ ,  $B_2$ , and  $B_5$  films, normalized by their peak values at 535–540 nm. Dashed lines indicate PL peak positions of noninteracting ADT-TES-F molecules and ADT-TES-F aggregates in a  $P_1$  film and of noninteracting ADT-TES-F molecules in a  $B_2$  film. Inset shows PL spectra from pristine ADT-TES-F film plotted with the aggregate PL spectra from  $P_1$  and  $B_1$ . (b) Normalized time-resolved PL decays in  $P_{10}$ ,  $P_3$ ,  $P_1$ , and pristine ADT-TES-F films. Lines correspond to a single-exponential fit in  $P_{10}$  and biexponential fits in other films. Instrument response function (IRF) is also included.

contributions both from noninteracting ADT-TES-F molecules and from ADT-TES-F aggregates can be seen in the PL spectra of  $P_2$ ,  $B_2$ , and  $P_1$  films. Inset of Fig. 2(a) shows PL spectra of aggregates in  $P_1$  and  $B_1$  films, obtained by subtraction of the portion of PL spectra due to noninteracting molecules (taken here as normalized PL spectra measured in  $P_{15}$  and  $B_{10}$  films for PMMA and t-bu BTBTB films, respectively) from the total PL spectra. Spectra of the aggregates in the  $P_1$  and  $B_1$  films, as well as in films with lower guest concentrations, were similar to those from a pristine ADT-TES-F film [inset of Fig. 2(a)], which suggests similar nature of the aggregates in all films. More studies, however, are needed to establish the exact type of these aggregates, as their optical and PL properties exhibit features of both H- and J-aggregates.<sup>9</sup> The PL spectral changes upon aggregation were accompanied by a change from a single-exponential decay with a lifetime of  $\sim 10\text{--}13 \text{ ns}$  to biexponential PL decays with lifetimes of  $\sim 2\text{--}3 \text{ ns}$  and  $\sim 8\text{--}13 \text{ ns}$ , with a contribution of the shorter lifetime increasing as the concentration of the guest molecule increased [Fig. 2(b)]. For example, in biexponential PL decays in  $P_3$ ,  $P_1$ , and pristine ADT-TES-F films in Fig. 2(b), the shorter lifetime, which we attribute to ADT-TES-F aggregates,<sup>12</sup> had relative weights of 0.44, 0.78, and 0.96, respectively. From absorption and PL spectra of films, we estimated a radiative lifetime of 11.4 ns and PL QY of 0.23 in ADT-TES-F aggregates.<sup>23</sup> Similarity between radiative lifetimes of ADT-TES-F aggregates and of noninteracting ADT-TES-F molecules (13.4 ns) (Ref. 5) suggests that aggregation enables nonradiative decay pathways which reduce PL QYs without significantly impacting radiative processes.

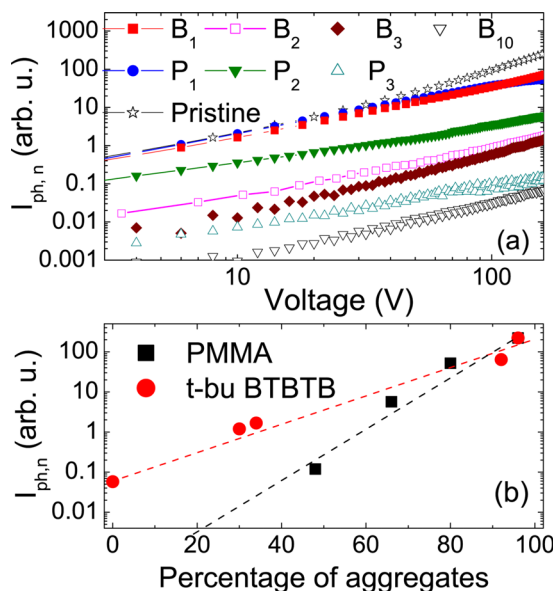


FIG. 3. (Color online) Photocurrent normalized by the number of absorbed photons,  $I_{ph,n}$ , measured at 5 mW/cm<sup>2</sup> 532 nm cw illumination: (a) as a function of applied voltage in B<sub>10</sub>, P<sub>3</sub>, B<sub>3</sub>, P<sub>2</sub>, B<sub>2</sub>, P<sub>1</sub>, B<sub>1</sub>, and pristine ADT-TES-F films and (b) at 150 V as a function of percentage of aggregated molecules calculated from the PL data from the same films. No aggregation (0%) was assumed for B<sub>10</sub>. Lines in (b) provide a guide for the eye.

The propensity for ADT-TES-F aggregation was significantly different in PMMA and t-bu BTBTB hosts. While 92% of ADT-TES-F molecules were in the aggregated state in a B<sub>1</sub> film, the percentage of aggregated molecules was only about 34% and 30% in B<sub>2</sub> and B<sub>3</sub> films, respectively. In contrast, 80%, 66%, and 48% of ADT-TES-F molecules were in the aggregated state in P<sub>1</sub>, P<sub>2</sub>, and P<sub>3</sub> films, respectively.<sup>23</sup> This suggests that structural similarity of ADT-TES-F guest and t-bu BTBTB host molecules provided effective dispersion of the ADT-TES-F guest molecules in the host matrix until high guest concentrations, in contrast to ADT-TES-F in PMMA. In films with  $r \geq 5$  nm, the percentage of aggregates was below 5% in both hosts.

For photocurrent measurements, samples were illuminated from the substrate side with  $\sim 5$  mW/cm<sup>2</sup> cw 532 nm light, which excited only ADT-TES-F molecules, and not t-bu BTBTB or PMMA. Currents in the dark and under photoexcitation as functions of applied voltage were measured using a Keithley 237 source-measure unit, and the photocurrent was calculated as the difference between the two. No photocurrent was observed upon excitation of pristine t-bu BTBTB or PMMA films. Figure 3(a) shows photocurrent normalized by the number density of absorbed photons ( $I_{ph,n}$ ) obtained in various films. Aggregate formation established via optical and PL measurements was correlated with an increase in the  $I_{ph,n}$  due to increase in charge carrier mobility in aggregates as compared to isolated guest molecules [Fig. 3(b)].<sup>24</sup> An increase in percentage of aggregated molecules in the P<sub>2</sub>(P<sub>1</sub>) with respect to the P<sub>3</sub> film led to a  $\sim 5$ -(45)-fold increase in the  $I_{ph,n}$ . B<sub>2</sub> and B<sub>3</sub> films, which had similar percentages of aggregates, had similar values of  $I_{ph,n}$ . These increased by a factor of  $\sim 70$  in the B<sub>1</sub> film that had a significantly higher percentage of aggregated molecules. At lower concentrations of ADT-TES-F guest molecules ( $r \geq 3$  nm), t-bu BTBTB films outperformed the PMMA ones [Fig. 3(b)],<sup>15</sup> most likely due to additional conductive pathways via t-bu BTBTB molecules.<sup>11</sup> These would contribute

if holes photoexcited on ADT-TES-F guest molecules overcame a  $\sim 0.4$  eV potential barrier between HOMO levels of ADT-TES-F and t-bu BTBTB, enabling charge transport in the t-bu BTBTB,<sup>15</sup> as evidenced by a detectable photocurrent in a B<sub>10</sub> film. In PMMA, conduction path through host molecules is inefficient, resulting in no measurable photocurrents in PMMA films at  $r \geq 5$  nm under our experimental conditions.

In summary, aggregation of ADT-TES-F guest molecules, quantified using optical and PL properties of films, was more pronounced in PMMA as compared to t-bu BTBTB host. Aggregates were characterized by redshifted optical absorption and PL spectra, as well as reduced PL QYs. Photocurrents dramatically increased as the aggregate content increased due to considerably higher charge carrier mobility in the ADT-TES-F aggregates. At low ADT-TES-F guest concentrations, t-bu BTBTB films exhibited significantly higher photocurrents than PMMA films due to additional conductive pathways via host molecules.

We thank M. Kendrick and G. Banton for technical assistance. This work was supported by NSF via CAREER program (Grant No. DMR-0748671).

- <sup>1</sup>H. E. Katz and J. Huang, *Annu. Rev. Mater. Res.* **39**, 71 (2009).
- <sup>2</sup>A. C. Arias, J. D. MacKenzie, I. McCulloch, J. Rivnay, and A. Salleo, *Chem. Rev. (Washington, D.C.)* **110**, 3 (2010).
- <sup>3</sup>S. K. Park, D. A. Mourey, S. Subramanian, J. E. Anthony, and T. N. Jackson, *Appl. Phys. Lett.* **93**, 043301 (2008).
- <sup>4</sup>D. J. Gundlach, J. E. Royer, S. K. Park, S. Subramanian, O. D. Jurchescu, B. H. Hamadani, A. J. Moad, R. J. Kline, L. C. Teague, O. Kirillov, C. A. Richter, J. G. Kushmerick, L. J. Richter, S. R. Parkin, T. N. Jackson, and J. E. Anthony, *Nature Mater.* **7**, 216 (2008).
- <sup>5</sup>A. D. Platt, J. Day, S. Subramanian, J. E. Anthony, and O. Ostroverkhova, *J. Phys. Chem. C* **113**, 14006 (2009).
- <sup>6</sup>J. Day, S. Subramanian, J. E. Anthony, Z. Lu, R. J. Twieg, and O. Ostroverkhova, *J. Appl. Phys.* **103**, 123715 (2008).
- <sup>7</sup>J. Day, A. D. Platt, O. Ostroverkhova, S. Subramanian, and J. E. Anthony, *Appl. Phys. Lett.* **94**, 013306 (2009).
- <sup>8</sup>S. Subramanian, S. K. Park, S. R. Parkin, V. Podzorov, T. N. Jackson, and J. E. Anthony, *J. Am. Chem. Soc.* **130**, 2706 (2008).
- <sup>9</sup>F. C. Spano, *Acc. Chem. Res.* **43**, 429 (2010).
- <sup>10</sup>O. D. Jurchescu, S. Subramanian, R. J. Kline, S. D. Hudson, J. E. Anthony, T. N. Jackson, and D. J. Gundlach, *Chem. Mater.* **20**, 6733 (2008).
- <sup>11</sup>L. B. Schein, D. S. Weiss, and A. Tyutnev, *Chem. Phys.* **365**, 101 (2009).
- <sup>12</sup>R. O. Al-Kaysi, T. S. Ahn, A. Muller, and C. J. Bardeen, *Phys. Chem. Chem. Phys.* **8**, 3453 (2006).
- <sup>13</sup>K. A. Colby, J. J. Burdett, R. F. Frisbee, L. Zhu, R. J. Dillon, and C. J. Bardeen, *J. Phys. Chem. A* **114**, 3471 (2010).
- <sup>14</sup>J. A. Hagen, W. Li, A. J. Steckl, and J. G. Grote, *Appl. Phys. Lett.* **88**, 171109 (2006).
- <sup>15</sup>W. E. B. Shepherd, A. D. Platt, G. Banton, M. A. Loth, J. E. Anthony, and O. Ostroverkhova, *Proc. SPIE* **7599**, 75990R (2010).
- <sup>16</sup>T. S. Ahn, N. Wright, and C. J. Bardeen, *Chem. Phys. Lett.* **446**, 43 (2007).
- <sup>17</sup>J. M. Giaimo, J. V. Lockard, L. E. Sinks, A. M. Scott, T. M. Wilson, and M. R. Wasielewski, *J. Phys. Chem. A* **112**, 2322 (2008).
- <sup>18</sup>P. J. Brown, D. S. Thomas, A. Kohler, J. S. Wilson, J. S. Kim, C. M. Ramsdale, H. Sirringhaus, and R. H. Friend, *Phys. Rev. B* **67**, 064203 (2003).
- <sup>19</sup>J. Clark, J. F. Chang, F. C. Spano, R. H. Friend, and C. Silva, *Appl. Phys. Lett.* **94**, 163306 (2009).
- <sup>20</sup>M. Pope and C. E. Swenberg, *Electronic Processes in Organic Crystals and Polymers*, 2nd ed. (Oxford University Press, New York, 1999).
- <sup>21</sup>F. C. Spano, *J. Chem. Phys.* **122**, 234701 (2005).
- <sup>22</sup>H. L. Cheng, W. Y. Chou, C. W. Kuo, Y. W. Wang, Y. S. Mai, F. C. Tang, and S. W. Chu, *Adv. Funct. Mater.* **18**, 285 (2008).
- <sup>23</sup>See supplementary material at <http://dx.doi.org/10.1063/1.3505493> for estimates of radiative lifetime and PL QYs of aggregates and example of calculation of relative percentages of aggregated and isolated molecules in films.
- <sup>24</sup>J. M. Sin and Z. G. Soos, *J. Chem. Phys.* **116**, 9475 (2002).